AIP | The Journal of Chemical Physics

Gas phase kinetics of the reactions of Na and NaO with O3 and N2O

Joel W. Ager III, Carol L. Talcott, and Carleton J. Howard

Citation: The Journal of Chemical Physics **85**, 5584 (1986); doi: 10.1063/1.451573
View online: http://dx.doi.org/10.1063/1.451573
View Table of Contents: http://scitation.aip.org/content/aip/journal/jcp/85/10?ver=pdfcov
Published by the AIP Publishing

Gas phase kinetics of the reactions of Na and NaO with O_3 and N_2O

Joel W. Ager III, Carol L. Talcott, and Carleton J. Howard[a)]
Aeronomy Laboratory, National Oceanic and Atmospheric Administration, Boulder, Colorado 80303 and Department of Chemistry and Biochemistry of the University of Colorado and Cooperative Institute for Research in Environmental Sciences, Boulder, Colorado

(Received 3 July 1986; accepted 5 August 1986)

A fast flow reactor, with an oven source and resonant fluorescence detection, was used to study the kinetics of Na atoms in the gas phase. The rate constant for $Na + O_3$ is $(7.3 \pm 1.4) \times 10^{-10}$ cm^3 molecule^{-1} s^{-1} at 286 K and $NaO + O_2$ is the predominant product channel. The rate constant for $Na + N_2O$ over the temperature range 240 to 429 K is $(3.7 \pm 0.9) \times 10^{-10} \exp[(-1690 \pm 180)/T]$ cm^3 molecule^{-1} s^{-1}. The kinetics of the NaO radical were measured directly. NaO is made in the flow tube by the reaction $Na + N_2O \rightarrow NaO + N_2$ with N_2O in large excess. NaO is detected by conversion to Na atoms in the detection region by $NaO + NO \rightarrow Na + NO_2$. $NaO + O_3$ has two exothermic product channels, $Na + 2O_2$ and $NaO_2 + O_2$. The rate constants are $\sim 5 \times 10^{-11}$ and $(1.8 \pm 0.4) \times 10^{-10}$ cm^3 molecule^{-1} s^{-1} at 296 K, respectively. Upper limits for $NaO + N_2O \rightarrow Na + N_2 + O_2$ and $NaO + N_2O \rightarrow NaO_2 + N_2$ are 1×10^{-16} and 2×10^{-15} cm^3 molecule^{-1} s^{-1}, respectively. The rate constant for $NaO + NO \rightarrow Na + NO_2$ is $\sim 1.5 \times 10^{-10}$ cm^3 molecule^{-1} s^{-1}. Since wall collisions remove NaO with near unit efficiency, NaO diffusion coefficients can be measured. $D_{NaO,He} = 640 \pm 340$ cm^2 Torr s^{-1} and $D_{NaO,N_2O} = 48 \pm 24$ cm^2 Torr s^{-1} at 295 K. The error limits in all cases represent the 95% confidence level, including an estimate of systematic errors.

I. INTRODUCTION

The reaction of Na atoms with ozone to form NaO, reaction (1a), was proposed by Chapman[1] in 1938 as one step in a catalytic cycle, consisting of reactions (1a), (2), and (3), to explain the Na *D* line night air glow emanating from the upper mesosphere:

$$Na + O_3 \rightarrow NaO + O_2, \quad \Delta H^\circ_{298} = -35 \text{ kcal mol}^{-1} \tag{1a}$$

$$\rightarrow NaO_2 + O, \quad \Delta H^\circ_{298} = -14 \text{ kcal mol}^{-1}, \tag{1b}$$

$$NaO + O(^3P) \rightarrow Na(^2P) + O_2, \quad \Delta H^\circ_{298} = -10 \text{ kcal mol}^{-1}, \tag{2}$$

$$Na(^3P) \rightarrow Na(^2S) + h\nu(590 \text{ nm}). \tag{3}$$

In 1964 Blamont and Donahue[2] estimated a rate constant of 6.5×10^{-12} cm^3 molecule^{-1} s^{-1} for reaction (1a) based on an analogy with $H + O_3$. In 1975 Kolb and Elgin[3] proposed that the electron jump model[4] can be applied to reactions (1a) and (2) and estimated a much faster rate constant of 3.3×10^{-10} cm^3 molecule^{-1} s^{-1} for reaction (1a), using the available value of the electron affinity of O_3.

The reaction of Na with O_3 has two exothermic product channels, (1a) and (1b). The rate constant for the sum of these channels was recently measured in a flow tube experiment by Silver and Kolb,[5] who obtained $k_1 = (3.1 \pm 0.4) \times 10^{-10}$ cm^3 molecule^1 s^{-1}, a value very close to the electron jump model estimate.[3] Husain *et al.*[6] have recently reported $k_1 = 4(+4, -2) \times 10^{-10}$ cm^3 molecule^{-1} s^{-1} from a flash photolysis study at 500 K. The product branching ratio was not measured in either study.

The reaction of Na with N_2O, reaction (4), is important in the

$$Na + N_2O \rightarrow NaO + N_2, \quad \Delta H^\circ_{298} = -21 \text{ kcal mol}^{-1} \tag{4}$$

catalyzed oxidation of CO to CO_2.[7] This oxidation scheme has been used to produce a CO_2 chemical laser.[8] The reaction is also useful as a source of NaO radicals in kinetic studies. The rate constant of reaction (4) was first measured in 1937 by Bawn and Evans[9] who used the diffusion flame technique and obtained $(2 \pm 1) \times 10^{-11}$ cm^3 molecule^{-1} s^{-1} at 535 K. In 1973 Walker and Creeden[10] measured a rate constant of 1.3×10^{-12} cm^3 molecule^{-1} s^{-1} at 330 K using a flow tube technique very similar to that used by Silver and Kolb[5] and in the present study. Silver and Kolb[5] obtained a rate constant of $(7.7 \pm 0.9) \times 10^{-13}$ cm^3 molecule^{-1} s^{-1} at 295 K. Recently, Husain and Marshall[11] have measured the temperature dependence of reaction (4) over the range 349 to 917 K in a flash photolysis/resonant absorption experiment and obtained $k_4 = (1.9 \pm 0.3) \times 10^{-10} \exp[(-1500 \pm 70)/T]$ cm^3 molecule^{-1} s^{-1}.

Very little is known about the spectroscopy of the NaO radical. There have been no published microwave, infrared, or matrix isolation studies. One chemiluminescence study[12] used reaction (4) under single collision conditions to produce visible emission which was attributed to NaO*. A problem with this assignment is that it is ~ 13 kcal mol^{-1} endothermic for reaction (4) to produce the observed emission. The heat of formation of NaO was measured in a mass spectroscopy study of the vaporization of Na_2O by Hildenbrand and Murad[13] who obtained $\Delta H^\circ_{f,298}(NaO) = 24.3 \pm 4.0$ kcal mol^{-1}.

[a)] Author to whom correspondence should be addressed at: NOAA R/E/A12, 325 Broadway, Boulder, CO 80303.

Theoretical studies[14–16] have predicted that $\Delta H^\circ_{f,298}$ (NaO) is in the range 25–27 kcal mol^{-1}. We have used the value of 24.8 ± 1.0 kcal mol^{-1} suggested by the review of Lamoreaux and Hildenbrand[17] in calculating the reaction enthalpies.[18] The calculated[16] bond length of 2.05 Å and dipole moment of 8.7 D correspond to 90% ionic character in the NaO bond.

The reactions of NaO with both O_3 and N_2O have two exothermic product channels:

$$NaO + O_3 \rightarrow Na + 2O_2, \quad \Delta H^\circ_{298} = -33 \text{ kcal mol}^{-1} \quad (5a)$$

$$\rightarrow NaO_2 + O_2, \quad \Delta H^\circ_{298} = -72 \text{ kcal mol}^{-1}, \quad (5b)$$

$$NaO + N_2O \rightarrow Na + N_2 + O_2, \quad \Delta H^\circ_{298} = -19 \text{ kcal mol}^{-1} \quad (6a)$$

$$\rightarrow NaO_2 + N_2, \quad \Delta H^\circ_{298} = -58 \text{ kcal mol}^{-1}. \quad (6b)$$

Silver and Kolb[5] reported $k_{5a} + k_{5b} = 2\times 10^{-10}$ cm^3 molecule^{-1} s^{-1}and $k_{5a}/k_5 = 0.7 \pm 0.2$ from modeling the effects of secondary chemistry in their flow tube.

This work describes direct room temperature measurements of the rate constant and the branching ratio for Na + O_3 and the temperature dependence of Na + N_2O over the range 240 to 429 K. We describe a method to perform direct kinetic studies of NaO radical and report rate constants for reactions (5b) and (6b).

II. EXPERIMENTAL

The Na oven source, the flow tube reactor, and the resonant fluorescence detection scheme are described in detail elsewhere.[19] The method for measuring Na atom rate constants is identical to that used in our previous work.[19]

Some minor modifications were made to the experimental apparatus in order to study NaO kinetics. The radical source is reaction (4), where N_2O is added to the flow tube with the carrier gas at the upstream flange. Although reaction (4) is not rapid, $k_4 = (1.0 \pm 0.2)\times 10^{-12}$ cm^3 molecule^{-1} s^{-1} at 292 K, enough N_2O is added to ensure that the reaction is essentially complete within a few cm downstream of the Na inlet tip. Under typical experimental conditions, $[N_2O] = 6.6\times 10^{15}$ molecule cm^{-3} and flow velocity $= v = 2000$ cm s^{-1}, the first-order rate constant for reaction (4) is 6600 s^{-1} and the conversion of Na to NaO is 99.8% complete 3 cm downstream of the Na inlet. NaO is detected by chemical conversion to Na via reaction (7),

$$NaO + NO \rightarrow Na + NO_2, \quad \Delta H^\circ_{298} = -12 \text{ kcal mol}^{-1}, \quad (7)$$

by addition of a large excess of NO through a gas inlet located 4 cm upstream of the Na resonant fluorescence detection region. We estimate the rate constant of reaction (7) to be about 1.5×10^{-10} cm^3 molecule^{-1} s^{-1} (see Sec. III). At a typical NO concentration of 1×10^{14} molecule cm^{-3} in the detection region, the first-order rate constant for reaction (7) is about 1.5×10^4 s^{-1}. Under these typical conditions Na and NaO go quickly to steady state by reactions (4) and (7). In the example given, roughly 70% of the NaO is converted to Na in the detection region. The Na and NaO radical concentrations are typically 10^4–10^7 molecule cm^{-3}, so reactions between Na species are negligible. The detection region chemistry is first-order, and the Na signal varies linearly with [NaO], regardless of the conversion efficiency. This was shown to be true by numerical simulation of the detection region chemistry. In an actual experiment, the amount of added NO is adjusted to optimize the Na signal, which involves a tradeoff between NaO conversion and fluorescence quenching by NO. We estimate that the detection limit for NaO is about the same as it is for Na, $\sim 1\times 10^4$ molecule cm^{-3}. To insure that this detection method is specific for NaO, an upper limit of 1×10^{-14} cm^3 molecule^{-1} s^{-1} was measured for the reaction of NaO_2 with NO,

$$NaO_2 + NO \rightarrow NaO + NO_2, \quad \Delta H^\circ_{298} = +25 \text{ kcal mol}^{-1}, \quad (8)$$

using Na + O_2 + He as the NaO_2 source in the flow tube. We expect this reaction to be much slower than this limit because it is very strongly endothermic.

In the measurement of the NaO + O_3 rate constant, chemiluminescence was observed from the reaction $NO + O_3 \rightarrow NO_2{}^* + O_2$ in the detection region. This background signal, which was comparable in magnitude to the scattered light, was subtracted from the total photocurrent.

This arrangement allows direct quantitative measurements of NaO kinetics, except for reactions in which Na is a product, such as reactions (5a) and (6a). In those cases the Na product reacts with the large excess of N_2O to regenerate NaO. Such product channels are detected by observing an Na signal with the NO off.

The O_3 used in this work was produced by an electrical discharge in pure O_2 and stored on silica gel at 195 K. The measured purity of the O_3 was ~90%, with the balance being O_2. At a flow tube pressure of 0.5 Torr of He, the ratio of the first-order rate constant for reaction (1) to that of reaction (9) is 2×10^5, so reaction (9) has no effect on the observed Na kinetics,

$$Na + O_2 + M \rightarrow NaO_2 + M, \quad \Delta H^\circ_{298} = -39 \text{ kcal mol}^{-1}. \quad (9)$$

For kinetic experiments the O_3 was eluted from the trap by a small (~0.5 STP cm^3 s^{-1}; STP = 760 Torr, 273 K) flow of helium. The partial pressure of O_3 in the He/O_3 flow was measured by absorption in a 10 cm pathlength cell at the 254 nm Hg line using an O_3 absorption cross section[20] of 1.15×10^{-17} cm^2. The He/O_3 mixture was added to the flow tube at the upstream flange. [O_3] was also measured at the detector end of the flow tube by UV absorption along a 17 cm transverse length. Both measurements agreed to within 4%. This measurement is a test of all flow and pressure calibrations and demonstrations that O_3 is not lost on the Na coated reactor wall.

The carrier gas in all the experiments was He (> 99.9%) purified over 50% 5*x*, 50% 13*x* molecular sieve at 78 K. Na reactions with carrier gas impurities have been shown to be completely negligible.[19,21] The NO (> 99%) was purified over silica gel at 195 K to remove NO_2 and other impurities. Preliminary measurements of the kinetics of Na + N_2O were made with very high purity N_2O (> 99.998%). Later, a lower grade of N_2O (> 99.99%) was used with no change in the observed kinetics. HCl (> 99%) was used without purification.

III. Na KINETICS

Initial measurements of the Na + O_3 rate constant produced curved decay plots and curved k_I vs $[O_3]$ plots that varied with flow tube velocity (see Fig. 1). This behavior was attributed to reaction (5a) reforming Na. Numerical simulations of the kinetics showed (see Sec. V) that reactions (1), (5a), and (5b) could explain the observed kinetics. To eliminate the effects of this secondary chemistry, the Na + O_3 rate constant was measured in the presence of an NaO scavenger, HCl. We measured an upper limit for the rate constant of reaction (10) of 4×10^{-13} cm^3 $molecule^{-1}$ s^{-1}:

$$\mathrm{Na} + \mathrm{HCl} \rightarrow \mathrm{NaCl} + \mathrm{H}, \quad \Delta H^\circ_{298} = +4.4 \ \mathrm{kcal\,mol^{-1}}. \tag{10}$$

Silver *et al.*[22] have reported that the rate constant for NaO + HCl, reaction (11), is very large, $\sim 3\times10^{-10}$ cm^3 $molecule^{-1}$ s^{-1}. This reaction has two exothermic product paths, neither of which can reform Na by reaction with O_3:

$$\mathrm{NaO} + \mathrm{HCl} \rightarrow \mathrm{NaCl} + \mathrm{OH}, \quad \Delta H^\circ_{298} = -37 \ \mathrm{kcal\,mol^{-1}} \tag{11a}$$

$$\rightarrow \mathrm{NaOH} + \mathrm{Cl}, \quad \Delta H^\circ_{298} = -23 \ \mathrm{kcal\,mol^{-1}}. \tag{11b}$$

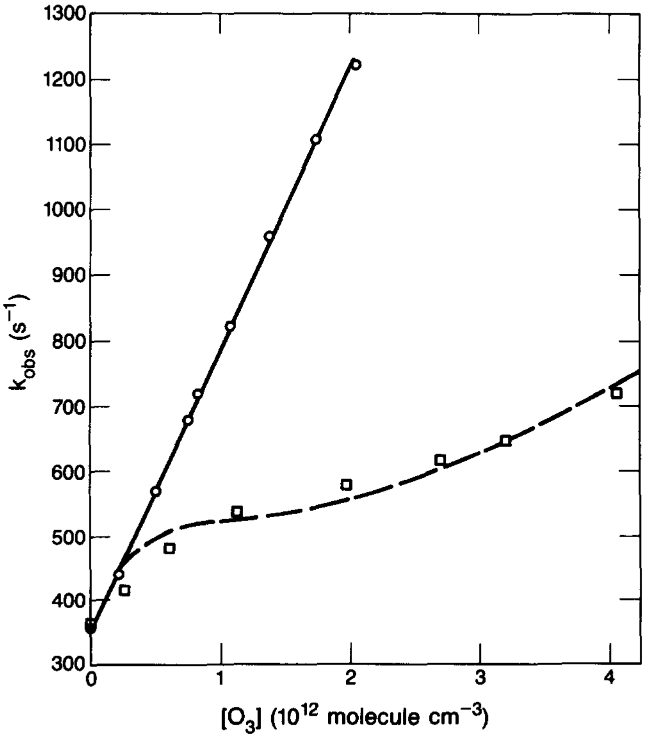

FIG. 1. k_{obs} vs $[O_3]$ for Na + O_3: (○) 0.522 Torr, $[HCl]/[O_3] > 4$, $v = 4200$ cm s^{-1}; (□) 0.522 Torr, [HCl] = 0, $v = 3900$ cm s^{-1}; (–) least squares fit to the scavenged system, $k_1 = (7.3 \pm 1.4)\times10^{-10}$ cm^3 $molecule^{-1}$ s^{-1}; (----) best fit to secondary chemistry, $k_{5a} = 5\times10^{-11}$ cm^3 $molecule^{-1}$ s^{-1}.

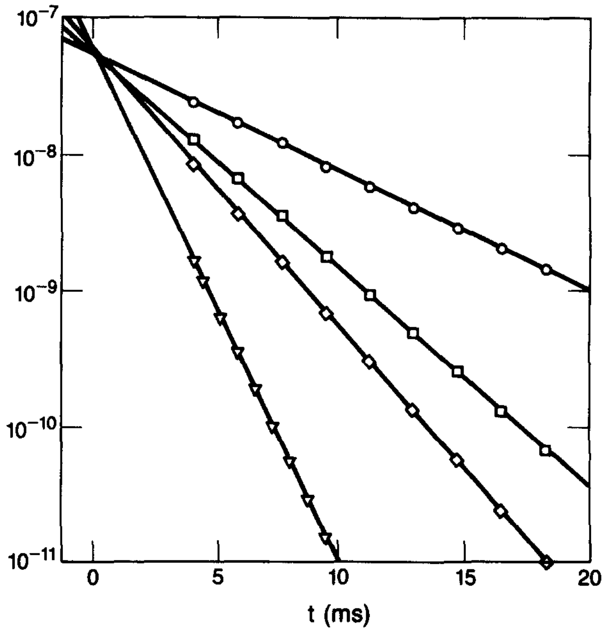

FIG. 2. Sample decay plots for Na + O_3 in the presence of HCl, 0.916 Torr, $v = 2750$ cm s^{-1}, 289 K: (○) $[O_3] = 0$, $[HCl] = 4.10\times10^{12}$ molecule cm^{-3}; (□) $[O_3] = 3.72\times10^{11}$ molecule cm^{-3}, $[HCl] = 6.53\times10^{12}$ molecule cm^{-3}; (◇) $[O_3] = 5.68\times10^{11}$ molecule cm^{-3}, $[HCl] = 1.13\times10^{13}$ molecule cm^{-3}; (▽) $[O_3] = 1.45\times10^{12}$ molecule cm^{-3}, $[HCl] = 1.47\times10^{13}$ molecule cm^{-3}.

Enough HCl was added to the flow tube through the upstream flange to ensure that reaction (11) would be the dominant loss process for NaO. The $[HCl]/[O_3]$ ratio was always larger than 4, so the first-order rate constant for reaction (11) was at least ten times faster than reaction (5a). Decay plots for the Na + O_3 reaction in the presence of HCl were linear as shown in Fig. 2. The k_I vs $[O_3]$ plots in the scavenged system showed no evidence of interfering secondary chemistry as shown in Fig. 1. The rate constant was independent of pressure and velocity over the ranges 0.30–1.5 Torr and 1800–8000 cm s^{-1}, respectively. The reaction rate constant was obtained from the observed first-order rate constant by the method of Brown[23] as described earlier.[19] The experimental data are tabulated in Table I. The rate constant for Na + O_3 is $(7.3 \pm 1.4)\times10^{-10}$ cm^3 $molecule^{-1}$ s^{-1}, where the error limits represent an estimate of random and systematic errors at the 95% confidence level. This is in excellent agreement with the results of a preliminary analysis of the unscavenged system which gave $k_1 \approx 6\times10^{-10}$ cm^3 $molecule^{-1}$ s^{-1} from the initial slopes of the decay plots.

The product distribution of the Na + O_3 reaction was evaluated by converting NaO formed by channel (1a) back to Na by adding NO to the flow tube. If channel (1b) were unimportant, large amounts of NO would drive all the product NaO back to Na via reaction (7). This will not be possible if channel (1b) were significant, since NaO_2 does not react appreciably with NO. Figure 3 summarizes the results of this type of experiment. At $[NO] = 3.5\times10^{12}$ molecule cm^{-3} and $[O_3] = 8.2\times10^{11}$ molecule cm^{-3}, the observed first-order loss of Na is indistinguishable from the wall loss. This means that reactions (1a) and (7) have reached steady state and that there is no evidence of channel (1b). We conclude from a modeling analysis of the kinetics that $k_{1a}/k_1 \geqslant 0.95$ and estimate that $k_7 \approx 1.5\times10^{-10}$ cm^3 $molecule^{-1}$ s^{-1}.

TABLE I. Na + O_3 kinetic measurements in the presence of HCl scavenger.

p (Torr)	No. of expts.	T (K)	v ($cm\ s^{-1}$)	[HCl]^a (10^{12} molecule cm^{-3})	[O_3] (10^{11} molecule cm^{-3})	$k_{II} \pm \sigma^b$ (10^{-10} cm^3 molecule^{-1} s^{-1})
0.299	6	283	8040	5.9	1.69–12.8	7.07 ± 0.09
0.522	9	289	4200	4.1–11	2.11–20.5	7.22 ± 0.07
0.576	9	289	6030	2.2–8.5	2.20–26.2	6.95 ± 0.08
0.687	7	283	3920	12	4.18–30.1	7.22 ± 0.21
0.916	9	289	2750	4.1–15	2.43–14.5	7.74 ± 0.07
1.56	5	283	1800	26	4.85–14.4	7.46 ± 0.16
					recommended value	$(7.3 \pm 1.4)^c$

[a] [HCl]/[O_3]>4 for all experiments.

[b] Otained from k_{obs} by the method of Brown (Ref. 23) as described in Ref. 19. The standard deviation is from the unweighted least squares fit of the data.

[c] The recommended value includes an estimate of random and systematic errors at the 95% confidence level.

The kinetics of Na + N_2O are less complex. A total of 93 measurements of the first-order decay were made. The second-order rate constant was measured 14 times at different pressures and velocities over the temperature range 240–429 K. Sample k_{obs} vs [N_2O] plots are shown in Fig. 4. The experimental results are summarized in Table II. The observed second-order rate constant at a given temperature shows no dependence on flow tube velocity or on the presence of the NaO scavenger, HCl. From these observations we conclude that the secondary reaction (6a) is much slower than reaction (4). By modeling reaction (4) and (6a) as a simple approach to equilibrium, we estimate $k_{6a} \leqslant 1 \times 10^{-16}$ cm^3 molecule^{-1} s^{-1} at 295 K. The Arrhenius plot is given in Fig. 5. The rate constant for Na + N_2O is $(3.7 \pm 0.8) \times 10^{-10} \exp[(-1690 \pm 180)/T]$ where the uncertainties are 2σ from the least squares fit.

Evidence for the endothermic reaction of Na with HCl, reaction (10), was observed at the highest temperatures. This cannot perturb the measurement of the primary reaction since in these experiments the concentration of HCl was kept constant over a series of runs; this is equivalent to having a larger Na wall loss.

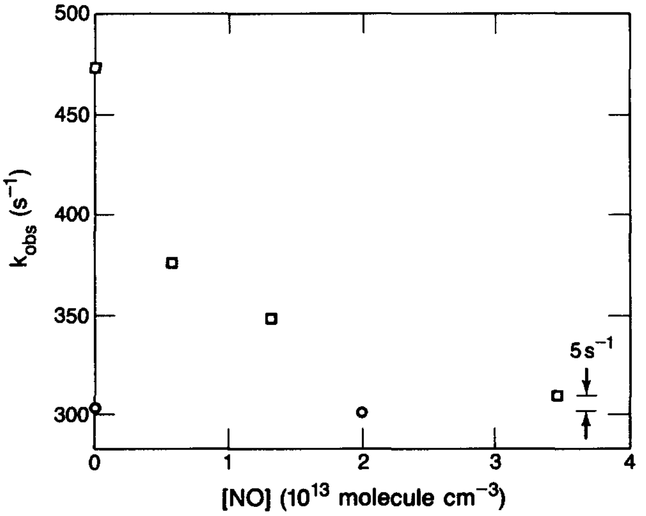

FIG. 3. Na + O_3 product branching ratio test (see Sec. III), 0.591 Torr, $v = 4030$ cm s^{-1}, 285 K: (○) [O_3] = 0; (□) [O_3] = 8.2×10^{11} molecule cm^{-3}; 5 s^{-1} is within the 3% measurement precision for k_{obs}.

IV. NaO KINETICS

The diffusion coefficient of NaO in the He and N_2O carrier gas mixture was measured by the method used previously.[19,21] The first-order wall loss rate was measured in 54 separate experiments over the pressure range 0.19–2.0 Torr at eight different mole fractions of N_2O. The k_{obs} vs p^{-1} plots were not linear and showed the behavior predicted[19,21] for simultaneous diffusion loss and reaction with a carrier gas component: $k_{obs} = ap^{-1} + bp$, where $a = 0.569\ D$ (D is the diffusion coefficient of NaO in the He/N_2O carrier gas mixture) and $b = 0.629\ k\ [C]$ (k is the bimolecular rate coefficient for the reactive component, C). The reactive component in this case is the N_2O itself and the reaction is

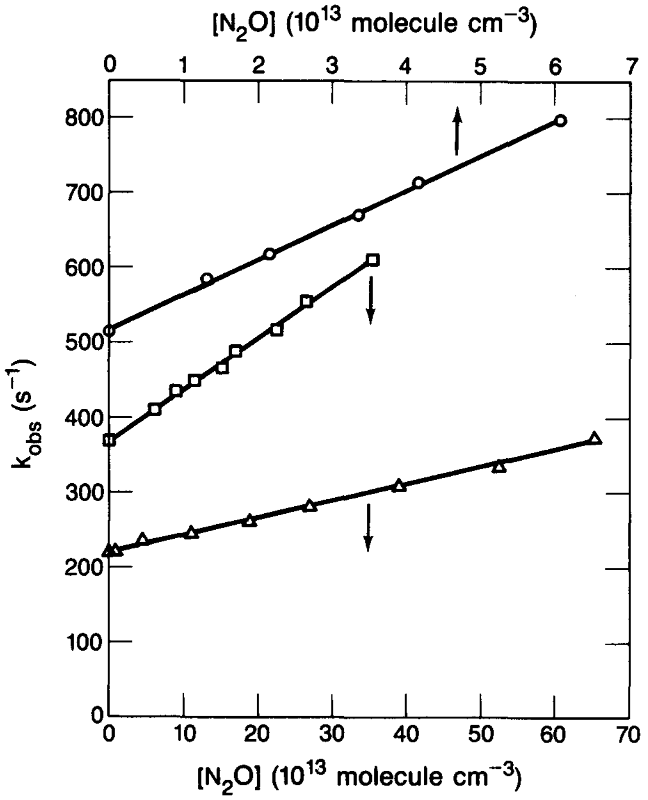

FIG. 4. Sample k_{obs} vs [N_2O] plots for Na + N_2O: (○) upper scale, 429 K, 0.770 Torr; (□) lower scale, 292 K, 0.544 Torr; (△) lower scale, 243 K, 0.656 Torr.

TABLE II. Na + N_2O kinetic data as a function of temperature.

T (K)	No. of expts.	p (Torr)	v (cm s^{-1})	[HCl] (10^{12} molecule cm^{-3})	[N_2O] (10^{13} molecule cm^{-3})	$k_{II} \pm \sigma^a$ (10^{-13} cm^3 $molecule^{-1}$ s^{-1})
240	6	1.23	1040	0	7.36–54.2	3.60 ± 0.07
243	9	0.656	2580	7.8	1.46–65.4	3.69 ± 0.05
256	6	1.33	1050	0	5.04–27.2	5.48 ± 0.02
273	6	1.44	1170	0	6.56–26.8	7.49 ± 0.03
291	6	0.790	1730	4.4	2.32–16.9	10.2 ± 0.5
292	9	0.544	2830	2.6	5.88–35.5	11.3 ± 0.3
292	6	0.830	1820	0	1.71–14.9	9.53 ± 0.32
293	6	1.47	950	0	8.60–13.3	11.6 ± 0.4
329	6	1.37	1380	0	3.07–17.0	21.6 ± 0.5
356	6	0.680	2350	0	1.79–9.70	28.2 ± 1.1
385	6	0.780	2670	0	0.919–6.31	47.1 ± 2.5
415	6	1.46	1370	1.5	1.88–6.99	65.7 ± 2.6
416	9	0.487	4470	0	0.555–6.97	65.4 ± 2.4
429	6	0.770	2530	0	1.29–6.07	82.6 ± 1.7
					$k_{II} = (3.7 \pm 0.9) \times 10^{-10} \exp[-1690 \pm 180)/T]^b$	

[a] Obtained from k_{obs} by the method of Brown (Ref. 23) as described in Ref. 19. The standard deviation is from the unweighted least squares fit of the data.

[b] The uncertainties are 95% confidence limits.

NaO + $N_2O \rightarrow NaO_2 + N_2$, reaction (6b). With this analysis, a plot of $k_{obs}p$ vs p^2 is linear, with a slope of b and a $p = 0$ intercept of a. A typical plot of this type is shown in Fig. 6 and is indeed linear. The rate constant for the NaO reaction with the carrier gas component is obtained from the slope of this plot. The measured rate coefficient was dependent on the N_2O reactant source, which indicates that NaO is also reacting with impurities in the N_2O. The slowest rates were obtained with electronic grade N_2O purified over molecular sieves at 213 K. Since we are not certain that the observed NaO reaction is due solely to N_2O, we report an upper limit for k_{6b} of 2×10^{-15} cm^3 $molecule^{-1}$ s^{-1}.

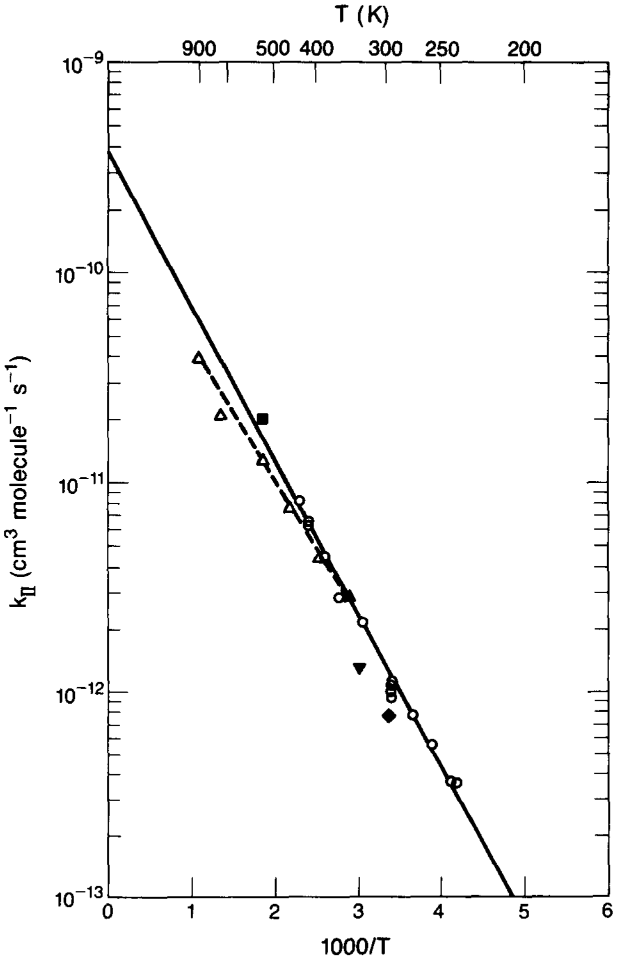

FIG. 5. Na + N_2O Arrhenius plot: (○) this work; (◆) Silver and Kolb (Ref. 5); (△) Husain and Marshall (Ref. 11); (▼) Walker and Creeden (Ref. 10); (■) Bawn and Evans (Ref. 9); (–) best fit to data of this work, $k_4 = (3.7 \pm 0.9) \times 10^{-10} \exp[(-1690 \pm 180)/T]$ cm^3 $molecule^{-1}$ s^{-1}; (----) fit to the data of Ref. 11.

The diffusion coefficient of NaO in the mixture of He and N_2O is obtained from the intercepts of the $k_{obs}p$ vs p^2 plots. Using the formula of Fairbank and Wilke[24] for minor component diffusion in a gas mixture, a plot of $D^{-1}_{NaO,\,He/N_2O}$ vs mole fraction N_2O, $f(N_2O)$, yields $D^{-1}_{NaO,\,He}$ as the $f(N_2O) = 0$ intercept and $D^{-1}_{NaO,\,N_2O}$ as the $f(N_2O) = 1$ val-

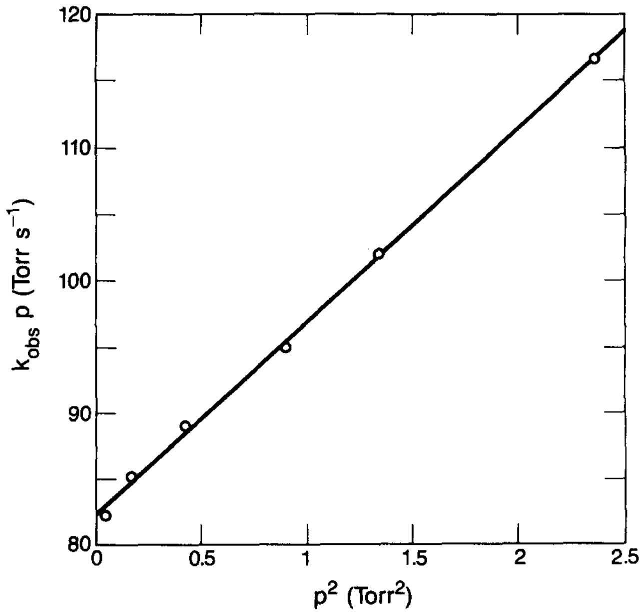

FIG. 6. NaO diffusion and reaction in 50.6% He/49.4% N_2O, $T = 295$ K, $D_{obs} \pm \sigma = 91.9 \pm 0.4$ cm^2 Torr s^{-1} and $k_{6b} \pm \sigma = (1.46 \pm 0.03) \times 10^{-15}$ cm^3 $molecule^{-1}$ s^{-1} are obtained from the intercept and slope, respectively, as described in Sec. IV.

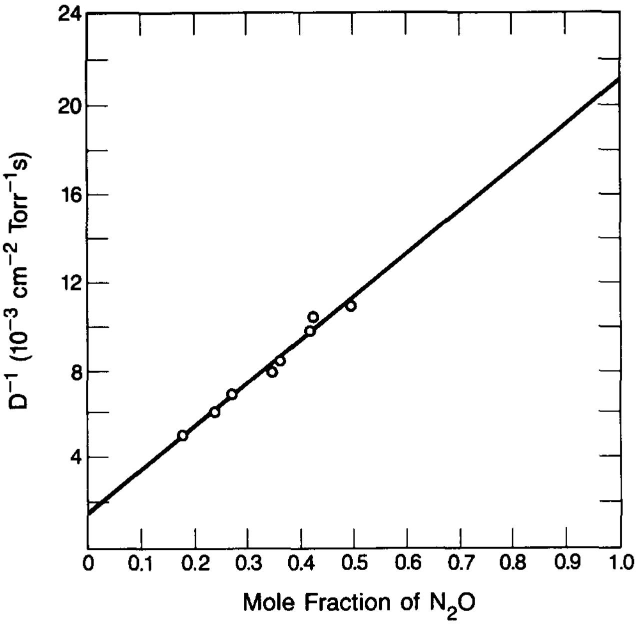

FIG. 7. $D^{-1}_{\mathrm{NaO,He/N_2O}}$ vs mole fraction of N_2O plot. The $f(N_2O) = 0$ and $f(N_2) = 1$ intercepts are $D^{-1}_{\mathrm{NaO,He}}$ and $D^{-1}_{\mathrm{NaO,N_2O}}$, respectively, as described in Sec. IV. $D_{\mathrm{NaO,He}} = 640 \pm 340$ cm^2 Torr s^{-1} and $D_{\mathrm{NaO,N_2O}} = 48 \pm 24$ cm^2 Torr s^{-1} where the error limits are 2σ from the least square fit.

ue. This plot is shown in Fig. 7. Our extrapolation yields $D_{\mathrm{NaO,He}} = 640 \pm 340$ cm^2 Torr s^{-1} and $D_{\mathrm{NaO,N_2O}} = 48 \pm 24$ cm^2 Torr s^{-1} at 295 K, where the error limits are 2σ from the least squares fit. Because the $[N_2O]$ and the pressure remain constant during the measurement of an NaO rate constant, the N_2O reaction does not disturb the kinetics measurement. Reaction (6b) is an added, but constant, first-order loss for NaO.

The rate constant for reaction (5b), $NaO + O_3 \rightarrow NaO_2 + O_2$, was directly measured using the NaO source and detection method described in the Experimental section. The NaO decay plots constructed by graphing the log of the Na signal from the converted NaO vs z are linear. The k_{obs} vs $[O_3]$ plots were also linear within the range discussed below as shown in Fig. 8. We identify two types of reaction processes in the $NaO + O_3$ system. Reactions (1a), (4), and (5a) establish the equilibrium between Na and NaO. Reaction (5b) and the wall losses of Na and NaO are permanent removal processes that convert Na species into unreactive forms. In the absence of O_3, the $[NaO]/[Na]$ ratio is very large since reaction (6b) goes quickly to completion and reaction (6a) has been shown to be slow. However, when $[O_3]$ is large, reaction (5a) converts some of the NaO to Na, thus lowering the $[NaO]/[Na]$ ratio. The Na produced by this equilibrium shift was directly observed with the NO off. It is observed that the k_{obs} vs $[O_3]$ plot curves down slightly at high $[O_3]$. This is caused by reaction (5a) converting the NaO, which has large permanent removal processes [wall and reaction (5b)] to Na, which has a smaller permanent loss process (just the wall). Numerical simulations of this system are discussed in Sec. V and show that this will cause a $< 5\%$ underestimate of the rate constant for reaction (5b).

Since the total first-order rate constants for NaO are smaller than their Na counterparts, axial diffusion, which was usually a $< 6\%$ effect in Na kinetics,[19] will be an even smaller effect in NaO kinetics. Therefore, the continuity equation solution of Huggins and Cahn,[25] which neglects axial diffusion, was used to extract the reaction rate constant from the experimental data. The experimental data are summarized in Table III. The rate constant for reaction (5b) is $(1.8 \pm 0.4) \times 10^{-10}$ cm^3 $molecule^{-1}$ s^{-1}, where the uncertainty limits include an estimate of random and systematic errors.

V. DISCUSSION

The $Na + O_3$ reaction proceeds by an electron jump mechanism as suggested by Kolb and Elgin.[3] The simple electron jump model[4] predicts a rate constant of 4.4×10^{-10} cm^3 $molecule^{-1}$ s^{-1} at 285 K, using $E.A.(O_3) = 2.103$ eV.[27] The refined electron jump model of Gislason[28] predicts a larger value, 6.1×10^{-10} cm^3 $molecule^{-1}$ s^{-1}, which is in good agreement with our measured value, $(7.3 \times 1.4) \times 10^{-10}$ cm^3 $molecule^{-1}$ s^{-1}. We expect charge transfer to be efficient, since the ozonide, $Na^+O_3^-$, is known to be the $Na + O_3$ reaction product in inert gas matrices.[26] In the gas phase the decomposition of this ionic reaction complex to $NaO + O_2$ is 35 kcal mol^{-1} exothermic, so we also expect this process to be efficient. Silver and Kolb[5] reported $k_1 = (3.1 \pm 0.4) \times 10^{-10}$ cm^3 $molecule^{-1}$ s^{-1} in a flow tube system very similar to the one used in the present study. Their result is only about half of the predicted collision rate constant. We do not know the reason for the large discrepancy between the two studies. Since we have had good agreement on the $Na + Cl_2$ rate constant[19] and on Na diffusion coefficients,[21] the measurement of $[O_3]$ may be a factor, although both studies exercised great care in measuring this reactant both outside and inside the flow reactor.

TABLE III. Kinetic data for the direct measurement of $NaO + O_3 \rightarrow NaO_2 + O_2$.

p (Torr)	No. of expts.	T (K)	v ($cm\ s^{-1}$)	Mole fraction of N_2O	$[O_3]$ (10^{11} molecule cm^{-3})	$k_{\mathrm{II}} \pm \sigma^{\mathrm{a}}$ (10^{-10} cm^3 $molecule^{-1}$ s^{-1})
0.364	9	296	7860	0.281	1.43–20.7	1.87 ± 0.09
0.560	4	296	4590	0.303	6.01–13.3	1.76 ± 0.13
0.845	8	296	2770	0.348	3.70–22.8	1.80 ± 0.06
1.28	8	296	3230	0.196	2.29–22.8	1.78 ± 0.03
					recommended value	$(1.8 \pm 0.4)^{\mathrm{b}}$

[a] Obtained from k_{obs} by the method of Brown (Ref. 23) as described in Ref. 19. The standard deviation is from the unweighted least squares fit of the data.
[b] The recommended value includes an estimate of random and systematic errors at the 95% confidence limit.

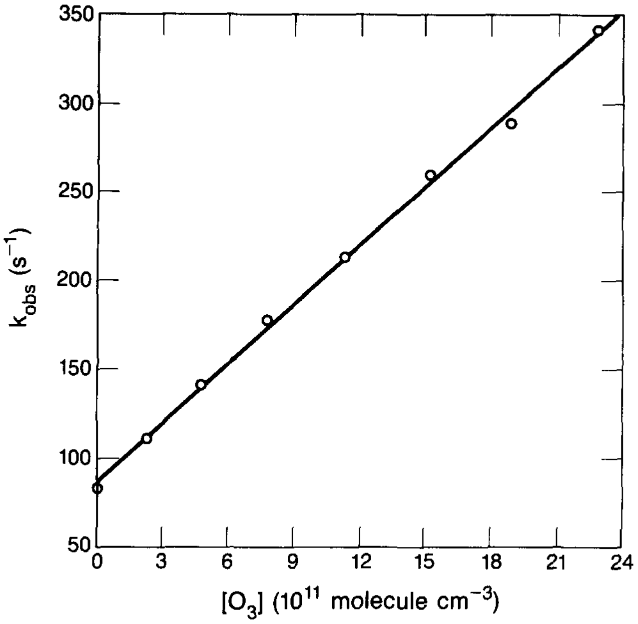

FIG. 8. Sample k_{obs} vs $[O_3]$ plot for $NaO + O_3 \rightarrow NaO_2 + O_2$, 1.28 Torr, $v = 3230$ cm s^{-1}, $[N_2O] = 8.19\times10^{15}$ molecule cm^{-3}, $k_{5b} = (1.8 \pm 0.4)\times10^{-10}$ cm^3 $molecule^{-1}$ s^{-1}.

Silver and Kolb[5] also used an NaO scavenger to reduce the effect of secondary chemistry. The value obtained by Husain *et al.*[6] at 500 K, $4(+4, -2)\times10^{-10}$ cm^3 $molecule^{-1}$ s^{-1}, is also significantly smaller than our measured value, although the results of both Silver and Kolb[5] and this work are within their uncertainty limits. Their value may be expected to be low, since no attempt was made to control the secondary chemistry of reaction (5a), which reforms the Na reactant.

The $Na + O_3$ reaction is the fastest reaction process for Na in the atmosphere at 90 km. Using our value for k_1, the results of Silver *et al.*[29] for $Na + O_2 + N_2$, an O_3 mixing ratio[30] of 1 ppm, and $T = 187$ K, the rate for the bimolecular Na reaction with O_3 is 15 times faster than the termolecular reaction with O_2 at 90 km.

The four previous measurements of the rate constant for $Na + N_2O$ are compared to this work in Table IV and Fig. 5. Our result is in good agreement with the early flame study of Bawn and Evans.[9] In their flow tube measurement of k_4, Walker and Creeden[10] observed Na D-line emission which they attributed to a chain reaction involving NaO. Since this chain reforms the Na reactant and would cause an underestimate of the rate constant, they multiplied their observed rate constant by a stoichiometry factor of 1.5 which was derived from an assumed mechanism. Their result is about 40% lower than ours. The source of the large discrepancy with the result of Silver and Kolb[5] is not known. Their result is about 35% lower than ours. The A factor obtained from the work of Husain and Marshall[11] over the range 349 to 917 K is $(1.9 \pm 0.3)\times10^{-10}$ cm^3 $molecule^{-1}$ s^{-1}, a factor of 2 smaller than the value obtained from our extrapolation. The activation energy measured in that study, (2.9 ± 0.1) kcal mol^{-1} is in good agreement with our value of (3.4 ± 0.4) kcal mol^{-1}, and their data extrapolated to 300 K is in perfect agreement.

Although it has a large uncertainty, we were initially surprised that our value for $D_{NaO,He}$, 640 ± 340 cm^2 Torr s^{-1}, is larger than our previously measured value for $D_{Na,He}$ of 380 ± 40 cm^2 Torr s^{-1}. A similar result was reported by Silver *et al.*[22] who found that $D_{NaOH,He} \approx D_{Na,He}$. From simple gas kinetic theory, the larger mass of NaO compared to Na would give a diffusion coefficient only 3% smaller for the same collision cross section.[31(a)] We expected $D_{NaO,He}$ to be smaller than $D_{Na,He}$ since the large dipole moment of NaO, 8.7 D, induces long range forces with the He. However, since the polarizability of He is small, 0.205 Å^3, this force is small compared to the dispersion attraction we estimate from a simple model,[31(b)]

$$C_6 = -\frac{3}{2}\left(\frac{I_1 I_2}{I_1 + I_2}\right)\alpha_1\alpha_2, \qquad (12)$$

where the I's are the ionization potentials[32] and the α's are the polarizabilities.[33] Since the polarizability of Na is large, $\alpha_{Na} = 23.6$ Å^3, compared to the value we estimate for NaO: $\alpha(Na^+) + \alpha(O^-) = 3.4$ Å^3,[34] the dispersion attraction in Na–He is actually larger than the sum of the dispersive and

TABLE IV. Comparison of measured $Na + N_2O$ rate constants.

Reference	Method[a]	T range (K)	k_{II}(300 K)[b] (cm^3 $molecule^{-1}$ s^{-1})
This work	oven source, flow tube, RF	240–429	$(1.3 \pm 0.2)\times10^{-12}$
Silver and Kolb[c]	oven source, flow tube, LIF	295	$(8.5 \pm 1.0)\times10^{-13}$
Husain and Marshall[d]	flash photolysis–resonant absorption	349–917	$(1.3 \pm 0.2)\times10^{-12}$
Walker and Creeden[e]	oven source, flow tube, RF	330	7.6×10^{-13}
Bawn and Evans[f]	diffusion flame	535	$(1.6 \pm 0.8)\times10^{-12}$

[a] RF, resonant fluorescence; LIF, laser induced fluorescence.
[b] Except when noted, extrapolated to 300 K by the temperature dependence measured in this work.
[c] Reference 5.
[d] Reference 11, extrapolation is that of the authors.
[e] Reference 10.
[f] Reference 9.

induced forces in NaO–He. On the other hand, the dipole-dipole induced dipole force is predominant in NaO–N_2O, which is consistent with the small measured diffusion coefficient, $D_{\mathrm{NaO, N_2O}} = 48 \pm 24$ cm^2 Torr s^{-1}.

The flow tube kinetics for the NaO + O_3 reaction were simulated with a computer model of the flow tube kinetics that includes Na and NaO reactions and diffusion to determine whether Na formation via reaction (5a) could perturb the direct measurement of k_{5b}. The simulations showed that k_{5b} could be accurately measured at low [O_3] and that the k_{obs} vs [O_3] plot would become significantly curved before an inaccurate estimate of k_{5b} would be made. For example, a simulation with $v = 4600$ cm s^{-1}, [N_2O] $= 5.5\times10^{15}$ molecule cm^{-3}, $k_1 = 7\times10^{-10}$ cm^3 molecule^{-1} s^{-1}, $k_{5a} = 1.5\times10^{-10}$ cm^3 molecule^{-1} s^{-1}, and $k_{5b} = 2\times10^{-10}$ cm^3 molecule^{-1} s^{-1} showed that for an [O_3] of up to 2×10^{12} molecule cm^{-3} only a 4% error would be made in the measurement of k_{5b}. The simulation also showed that Na and NaO are in steady state after 15 cm as was experimentally found by observing decays with the NO on and the NO off.

A measurement of Na + O_3 in the absence of scavenger gives a complex Na decay caused by reactions (1a), (5a), (5b), and diffusion. For this reason we could not quantitatively estimate the rate constants of reactions (5a) and (5b) by fitting the small curvature of the Na decay plots as was done by Silver and Kolb.[5] However, we can fit the k_{obs} vs [O_3] plots in the unscavenged experiments by simulating the decay with the computer model and calculating a first-order rate constant appropriate for the experimental time scale. The low velocity Na + O_3 experiments without scavenger were simulated using the measured values for k_1, k_4, k_{5b}, $D_{\mathrm{Na, He}}$, and $D_{\mathrm{NaO, He}}$. The simulation predicts that the slope of the k_{obs} vs [O_3] plot at large [O_3] will be k_{5b}. Taking these slopes from three low velocity Na + O_3 experiments we estimate $k_{5b} \approx 1.5\times10^{-10}$ cm^3 molecule^{-1} s^{-1}. This is in excellent agreement with the directly measured value. The best fit to these data was obtained for $k_{5a} \approx 5\times10^{-11}$ cm^3 molecule^{-1} s^{-1}. A sample fit is shown in Fig. 1. The simulation accurately reproduces the shape of the experimental plot, especially the flat region at moderate [O_3].

Since the source reaction for NaO is 25 kcal mol^{-1} exothermic we must consider the possibility of excited NaO, especially the low lying[14] $A\,^2\Sigma$ state at $\sim$2200 cm^{-1}. The vibrational and electronic relaxation of NaO by collisions is expected to be fast because the dipole moments of both the ground and excited electronic state are large[16] (8.7 D) which leads to large long-range interactions with the carrier gases, especially N_2O. The electronic relaxation is also expected to be fast, since the $A\,^2\Sigma \rightarrow X\,^2\Pi$ transition is optically allowed. A lower limit for the radiative lifetime can be calculated by assuming that the oscillator strength of the transition is unity and this calculation yields $\tau \geqslant 0.3$ μs. A much longer lifetime on the order of a few ms is necessary for the $^2\Sigma$ state to perturb the kinetics. At a typical flow tube pressure of 0.3 Torr and a velocity of 2000 cm s^{-1} the excited NaO would have to survive about 1×10^4 collisions, many of which would be with N_2O, to travel 10 cm. We feel this is unlikely. If our NaO reactant were a mixture of ground state and excited species with different reactivities, we would expect to find curved decay plots and velocity and pressure dependences in the NaO rate constant. These effects were not experimentally observed. We conclude that the reported kinetic data represent reaction of a thermal distribution of ground state NaO.

Our directly measured value for the rate constant of NaO + $O_3 \rightarrow NaO_2 + O_2$ of $(1.8\pm0.4)\times10^{-10}$ cm^3 molecule^{-1} s^{-1} is in good agreement with the indirect measurement of Silver and Kolb[5] of $\sim1.4\times10^{-10}$ cm^3 molecule^{-1} s^{-1}. The indirectly measured values for NaO + $O_3 \rightarrow$ Na + $2O_2$ obtained by this work and Silver and Kolb[5] are also in good agreement, $\sim5\times10^{-11}$ and $\sim6\times10^{-11}$ cm^3 molecule^{-1} s^{-1}, respectively. In contrast to Na + O_3, it is interesting that there is no discrepancy with Silver and Kolb[5] on these O_3 reactions. The refined electron jump model[28] predicts a rate constant for both channels of the NaO + O_3 reaction of 4.0×10^{-10} cm^3 molecule^{-1} s^{-1} using I.P.(NaO) = 6.5 eV from Hildenbrand and Murad.[13] This is somewhat larger than the sum of the experimental values for k_{5a} and k_{5b}.

Further work on the reactions of NaO with H_2, H_2O, hydrocarbons, and alcohols is in progress.

ACKNOWLEDGMENTS

We thank Mr. Eugene Boe for his assistance in developing the computer programs used in the numerical simulations. This work was supported in part by the Chemical Manufacturers Association Technical Panel on Fluorocarbon Research.

[1] S. Chapman, Astrophys. J. **90**, 309 (1939).
[2] J. E. Blamont and T. M. Donahue, J. Geophys. Res. **69**, 4093 (1964).
[3] C. E. Kolb and J. B. Elgin, Nature (London) **263**, 488 (1976).
[4] R. D. Levine and R. B. Bernstein, *Molecular Reaction Dynamics* (Oxford University, New York, 1974), p. 87.
[5] J. A. Silver and C. E. Kolb, J. Phys. Chem. **90**, 3263 (1986).
[6] D. Husain, P. Marshall, and J. M. C. Plane, J. Chem. Soc. Chem. Commun. **18**, 1216 (1985).
[7] C. P. Fenimore and J. R. Kelso, J. Am. Chem. Soc. **72**, 5045 (1950).
[8] R. C. Benson, C. B. Burgeron, and R. E. Walker, Chem. Phys. Lett. **35**, 161 (1975).
[9] C. E. H. Bawn and A. G. Evans, Trans. Faraday Soc. **33**, 1571 (1937).
[10] R. E. Walker and J. E. Creeden, Combust. Flame **21**, 39 (1973).
[11] D. Husain and P. Marshall, Combust. Flame **60**, 81 (1985).
[12] J. Pfeifer and J. L. Gole, J. Chem. Phys. **80**, 565 (1984).
[13] D. L. Hildenbrand and E. Murad, J. Chem. Phys. **53**, 3403 (1970).
[14] J. N. Allison and W. A. Goddard III, J. Chem. Phys. **77**, 4259 (1982); J. N. Allison, R. J. Cave, and W. A. Goddard III, J. Phys. Chem. **88**, 1262 (1984).
[15] M. J. Clugston and R. G. Gordon, J. Chem. Phys. **66**, 244 (1977).
[16] P. A. G. O'Hare and A. C. Wahl, J. Chem. Phys. **56**, 4516 (1972).
[17] R. H. Lamoreaux and D. L. Hildenbrand, J. Phys. Chem. Ref. Data **13**, 151 (1984).
[18] We use $\Delta H^\circ_{f,298}(NaO_2) = -13 \pm 5$ kcal mol^{-1} from A. J. Hynes, M. Steinberg, and K. Schofield, J. Chem. Phys. **80**, 2585 (1984) and $\Delta H^\circ_{f,298}(NaOH) = -43.8 \pm 2.0$ kcal mol^{-1} from R. Kelly and P. J. Padley, Trans. Faraday Soc. **67**, 740 (1971). All other enthalpies of formation are from *JANAF Thermochemical Tables*, edited by D. R. Stull and H. Prophet, Natl. Bur. Stand. (U.S. GPO, Washington, D.C., 1971); compiled and calculated by the Dow Chemical Co., Midland, MI.
[19] C. L. Talcott, J. W. Ager III, and C. J. Howard, J. Chem. Phys. **84**, 6161 (1986).

[20] W. B. DeMore, J. J. Margitan, M. J. Molina, R. T. Watson, D. M. Golden, R. F. Hampson, M. J. Kurylo, C. J. Howard, and A. R. Ravishankara, *Chemical Kinetics and Photochemical Data for Use in Stratospheric Modeling*, Evaluation No. 7, Jet Propulsion Laboratory publication 85-37 (1985).

[21] J. W. Ager III and C. J. Howard, J. Chem. Phys. (in press).

[22] J. A. Silver, A. C. Stanton, M. S. Zahniser, and C. E. Kolb, J. Phys. Chem. **88**, 3123 (1984).

[23] R. L. Brown, J. Res. Natl. Bur. Stand. **83**, 1 (1978).

[24] D. F. Fairbank and C. R. Wilke, Ind. Eng. Chem. **42**, 471 (1950).

[25] R. W. Huggins and J. H. Cahn, J. Appl. Phys. **38**, 180 (1967).

[26] R. C. Spiker and L. Andrews, J. Chem. Phys. **59**, 1851 (1973); L. Andrews and R. C. Spiker, *ibid.* **59**, 1863 (1973).

[27] S. E. Novick, P. C. Engelking, P. L. Jones, J. H. Futrell, and W. C. Lineberger, J. Chem. Phys. **70**, 2652 (1979).

[28] E. A. Gislason, in *Alkali Halide Vapors*, edited by P. Davidovits and D. L. McFadden (Academic, New York, 1979), pp. 415–440.

[29] J. A. Silver, M. S. Zahniser, A. C. Stanton, and C. E. Kolb, in *20th Symposium (International) on Combustion* (The Combustion Institute, Pittsburgh, 1985), p. 605.

[30] R. J. Thomas, C. A. Barth, and S. Solomon, Geophys. Res. Lett. **11**, 673 (1984).

[31] J. O. Hirschfelder, C. F. Curtiss, and R. B. Bird, *Molecular Theory of Gases and Liquids* (Wiley, New York, 1954), (a) p. 539; (b) p. 963.

[32] Unless noted all ionization potentials are from H. M. Rosenstock, K. Draxl, B. W. Steiner, and J. T. Herron, J. Chem. Phys. Ref. Data **6**, Supplement No. 1 (1977).

[33] Unless noted all polarizabilities are from T. M. Miller, in *Handbook of Chemistry and Physics*, 66th ed., edited by R. C. Weast (Chemical Rubber, Boca Raton, 1985), pp. E-65–E-74.

[34] A. Dalgarno, Adv. Phys. **11**, 281 (1962).